Extraction of $A_{LU}^{\sin(\phi)}$ from the hard exclusive π^+ channel in a wide range of kinematics

Stefan Diehl[1,2] and Kyungseon Joo[2] for the CLAS collaboration

[1] 2nd Physics Institute, Justus Liebig University Giessen, 35392 Giessen, Germany
[2] University of Connecticut, Storrs, Connecticut 0626, USA

stefan.diehl@exp2.physik.uni-giessen.de

Abstract. The beam-spin asymmetry (BSA) has been measured for the hard exclusive e p → e n π^+ reaction over a wide range of kinematics in the deep inelastic regime. The measurements were performed with the CEBAF Large Acceptance Spectrometer (CLAS) using a 5.5 GeV polarized electron beam at Jefferson Lab (JLAB). The ϕ dependence of the BSA as well as the –t, Q^2 and x_B dependence of the extracted $A_{LU}^{\sin(\phi)}$ moment will be presented. For $A_{LU}^{\sin(\phi)}$ a clear sign change can be observed between pions emitted in forward and backward direction with a smooth transition around 90° in CM. The results will be discussed in the context of formalisms depending on generalized parton distributions (GPDs) and transition distribution amplitudes (TDAs), which can be used to describe complementary kinematic regimes.

1. Introduction

The investigation of the 3 dimensional nucleon structure in terms of spatial and momentum distributions is an important tool to understand the fundamental properties of the nucleon. Theoretically, the 3 dimensional nucleon structure is described by Wigner functions, which depend on the three dimensional coordinate distributions as well as the momentum distributions of the constituents. Experimentally coordinate and momentum can not be measured exactly at the same time. Therefore different formalisms and experimental methods are used to investigate them. On the one side, the distribution in momentum space is described by transverse momentum depended distribution functions (TMDs) which can be accessed by semi-inclusive deep inelastic processes in electron scattering experiments or Drell-Yan processes in particle-antiparticle annihilation experiments. On the other side, the spatial distribution is encoded in generalized parton distributions (GPDs), which are classically measured by deeply virtual Compton scattering (DVCS). While DVCS is a clean process, it is only sensitive to chiral even GPDs. The transversity degrees of freedom, described by the chiral-odd GPDs can be accessed by deeply virtual meson production, which also enables a flavor decomposition of GPDs.

GPDs are universal structure functions, which describe the hadronic structural information in terms of quark-gluon degrees of freedom. They are known to be a good tool to study the nature and the origin of the nucleon spin. In the impact parameter space, they can be interpreted as spatial femto-photographs of the nucleon structure in the transverse plane. In theory they have been extensively studied, see [1-10]. For the hard exclusive meson production, the collinear factorization theorem of

QCD allows a GPD based description for large Q^2 and s values and a small t channel contribution, which practically corresponds to a pion going in forward direction.

Besides the GPD based description the collinear factorization theorem also allows a description of the hard exclusive pion production by Transition Distribution Amplitudes (TDAs). TDAs encode a physical picture, which is very similar to that of GPDs. They are universal structure functions, which probe the partonic correlation between states of different baryonic charge and therefore give us access to non-minimal Fock components of the baryon light cone wave function. Interpreted in the impact parameter space, they allow a nuclear femto-photography from a new perspective and can provide a spatial image of the structure of the pion cloud inside the nucleon. The theoretical formalism is described in [11-15]. The TDA based description is valid for large Q^2 and s and for a small u channel transfer, which correspond to large -t values in the case of exclusive pion production. Therefore the TDAs and GPDs describe complementary kinematic regimes. Fig. 1 compares the GPD and the TDA based reaction mechanism for the hard exclusive pion production.

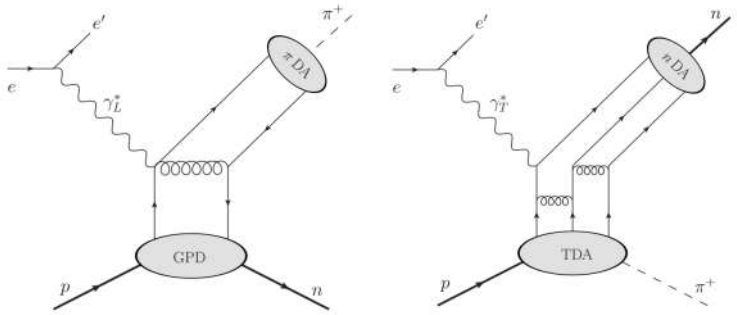

Figure 1. Schematic diagram for the exclusive e p → e n π^+ reaction for a GPD based description (left) and for a TDA based description (right).

The cross section of the hard exclusive reaction e p → e n π^+ is shown in Fig. 2. It depends on the virtuality $\boldsymbol{Q^2}$ and the transverse and longitudinal polarization (ε, ε_L) of the virtual photon as well as on Bjorken $\boldsymbol{x_B}$, the squared momentum transfer $\boldsymbol{t}$ to the proton and on the angle ϕ between the leptonic and the hadronic planes. Measurements of the cross section in backward kinematics have been performed in [16].

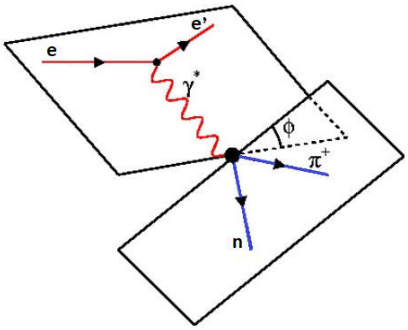

$$\frac{d\sigma}{d\Omega_{e'} d\epsilon_{e'} \Omega_\pi} = \Gamma \frac{d\sigma_\nu}{d\Omega_\pi} \qquad \Gamma = \frac{\alpha_{em}}{2\pi^2} \frac{E_{e'}}{E_0} \frac{W^2}{Q^2} \frac{1}{1-\epsilon}$$

$$\frac{d\sigma_\nu}{d\Omega_\pi} = \frac{d\sigma_T}{d\Omega_\pi} + \epsilon_L \frac{d\sigma_L}{d\Omega_\pi} + \sqrt{2\epsilon_L(1+\epsilon)} \frac{d\sigma_{TL}}{d\Omega_\pi} \cos(\phi)$$
$$+ \epsilon \frac{d\sigma_{TT}}{d\Omega_\pi} \cos(2\phi) + h\sqrt{2\epsilon_L(1-\epsilon)} \frac{d\sigma_{TL'}}{d\Omega_\pi} \sin(\phi)$$

Figure 2. Illustration of the electron scattering plane and the hadron production plane for the reaction ep → enπ^+ with the angle ϕ between the two planes. The cross section of the process, which depends besides the angle ϕ also on the beam polarization h, and the transverse, longitudinal, transverse-transverse and longitudinal-transverse interference structure functions (T, L, TT, TL, and TL′)

By substituting the terms in front of the ϕ dependences with the moments $A_{UU}^{\cos(\phi)}$, $A_{UU}^{\cos(2\phi)}$ and $A_{LU}^{\sin(\phi)}$ and a factor $d\sigma_0$, the cross section can be simplified to:

$$d\sigma = d\sigma_0 \cdot (1 + h \cdot A_{LU}^{\sin(\phi)} \sin(\phi) + A_{UU}^{\cos(\phi)} \cos(\phi) + A_{UU}^{\cos(2\phi)} \cos(2\phi)) \qquad (1)$$

Based on the three moments, which depend on Q^2, x_B and -t, the beam-spin asymmetry can be defined as:

$$BSA = \frac{\sigma^+ - \sigma^-}{\sigma^+ + \sigma^-} = \frac{A_{LU}^{\sin(\phi)} \sin(\phi)}{1 + A_{UU}^{\cos(\phi)} \cos(\phi) + A_{UU}^{\cos(2\phi)} \cos(2\phi)} \quad (2)$$

where σ± is the cross section for the two helicity states with the spin parallel (+) and anti-parallel (-) to the beam direction.

2. Experimental setup and particle identification

The analyzed data was recorded with the CEBAF Large Acceptance Spectrometer (CLAS) in hall B at Jefferson LAB in 2003, using a 5.5 GeV longitudinally polarized electron beam, interacting with an un-polarized hydrogen target. The average beam polarization was measured with a Moller polarimeter in the beam line upstream of CLAS as 74.9 ± 2.4(stat) %. The setup, as well as a picture of the CLAS detector is shown in Fig. 3.

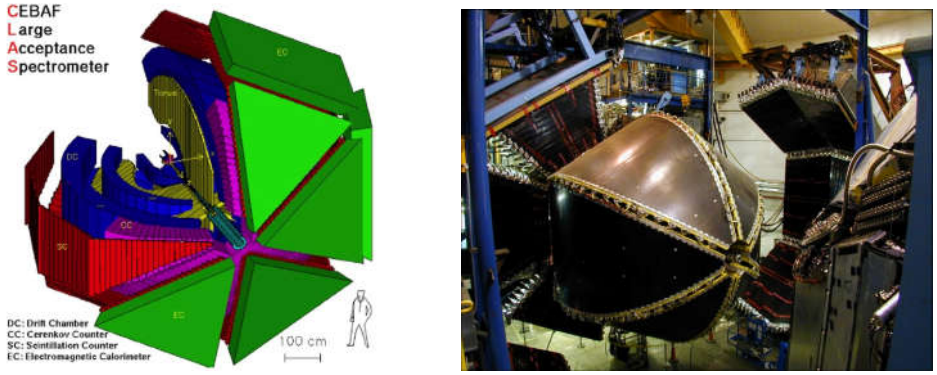

Figure 3. The CLAS detector in hall B at JLAB. Schematic drawing (left) and photograph of the detector setup (right)

The CLAS detector is build around a torus magnet, which divides the setup in six sectors. Each sector contains 3 regions of drift-chambers to determine the momentum of charged particles within the torus field, a Cherenkov counter and a time of flight system for the identification of charged particles and an electromagnetic calorimeter to identify electrons and to detect photons.

3. Analysis procedure

As a first step, events with deeply inelastic scattered electrons were selected with cuts on $Q^2 > 1$ GeV² and $W > 2$ GeV. To separate the forward and backward kinematic region, cuts on the Mandelstam variables t and u and on the polar angle θ_{CM} of the π^+ in the centre of mass frame were applied. The forward direction is defined as $-t < 1.5$ GeV² and $\cos(\theta_{CM}) > 0$. For the backward direction, cuts on $-u < 2.0$ GeV² and $\cos(\theta_{CM}) < 0$ are used. The Mandelstam variables t and u describe the momentum transfer between the virtual photon and the produced pion and between the initial target proton and the final state pion, respectively.

Since for the reaction $ep \rightarrow en\pi^+$ only electrons and pions can be detected by CLAS, the excusive events are selected by a cut on the missing neutron mass in $e\pi^+X$. The fitted missing neutron peak and its background are shown in Fig. 4. The fit has been performed for each kinematic bin to determine the signal to background ratio. The kinematic coverage of the exclusive events in Q^2, W and x_B is shown in Fig. 5.

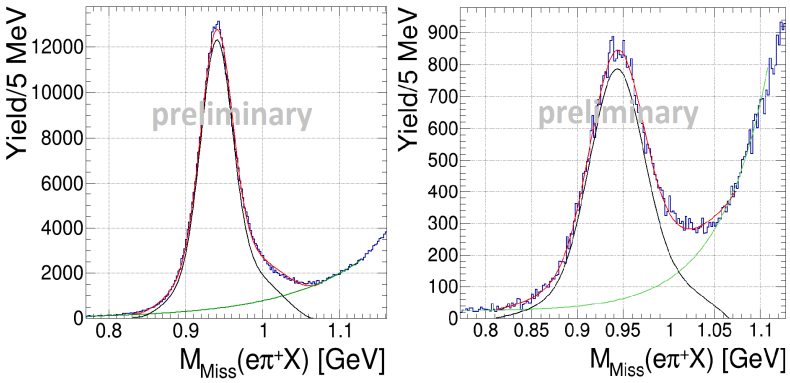

Figure 4. Missing mass of $e\pi^+X$ in the forward region (left) and in the backward region (right). The black line shows the signal and the green line the fitted background contribution.

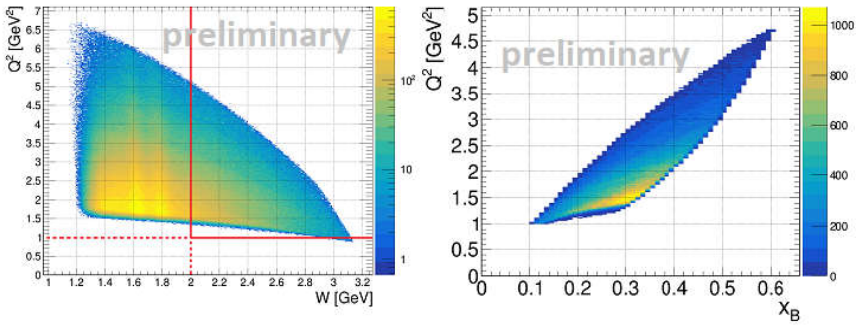

Figure 5. Kinematic coverage of the exclusive $ep \rightarrow en\pi^+$ events in Q^2, W and x_B. The red lines show the cuts which are placed on Q^2 and W to select the deep inelastic scattering region.

4. Results

Experimentally, the beam spin asymmetry can be calculated by equation 3.

$$BSA = \frac{1}{P_e} \frac{N_i^+ - N_i^-}{N_i^+ + N_i^-} \tag{3}$$

Where P_e is the average beam polarization and $N_i^{\pm}$ are the count rates in a specific bin with positive and negative helicity. The beam-spin asymmetry as a function of ϕ for the forward and backward kinematic region, integrated over Q^2 and x_B is shown in Fig. 6.

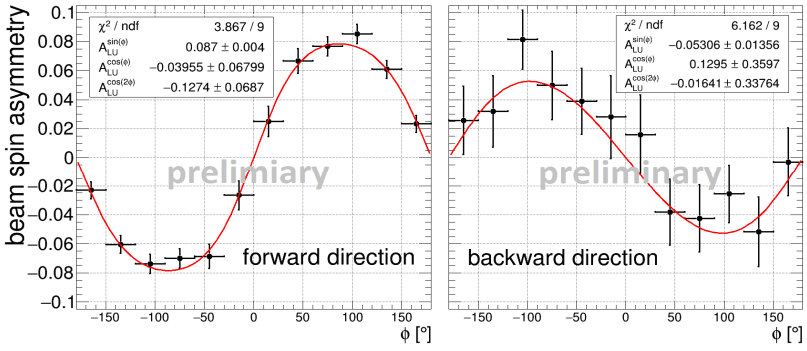

Figure 6. Beam spin asymmetry in forward (left) and backward direction (right). Both plots are integrated over all Q^2 and x_B bins. The shown result is preliminary.

The ϕ dependence is fitted with equation 2. A clear sign change of $A_{LU}^{\sin(\phi)}$ can be observed between the forward and backward kinematic region.

To investigate the transition between the forward and backward kinematics more closely, $A_{LU}^{\sin(\phi)}$ has been extracted for different bins in –t, Q^2 and x_B. By selecting a missing mass interval on the right side of the missing neutron peak in Fig. 4, the asymmetry of the background has been determined for each kinematic bin. It was found, that the background can be described by a sinoid shape, with an average $A_{LU}^{\sin(\phi)}$ value of 0.032 in the forward direction and 0.00 in the backward direction. Based on the signal to background ratio from the fit of the missing mass distribution, a background subtraction has been performed in each bin. The effect on the results is on a comparable level as the statistical uncertainty.

Besides the statistical uncertainty, also the systematic uncertainty has been investigated. Thirteen different sources of systematic uncertainty were considered, including the particle identification, the beam polarization and the influence of the $A_{UU}^{\cos(\phi)}$ and $A_{UU}^{\cos(2\phi)}$ moments. Each contributing source was varied around its nominal value to determine the maximal uncertainty. A fast MC simulation was used to determine the impact of acceptance effects, which was found to be negligible. Each source of systematic uncertainty stays well below the statistical uncertainty. The total systematic uncertainty is defined as the square root of the quadratic sum of all contributions. Fig. 7 shows the -t dependence of $A_{LU}^{\sin(\phi)}$ including the statistical and systematic uncertainty.

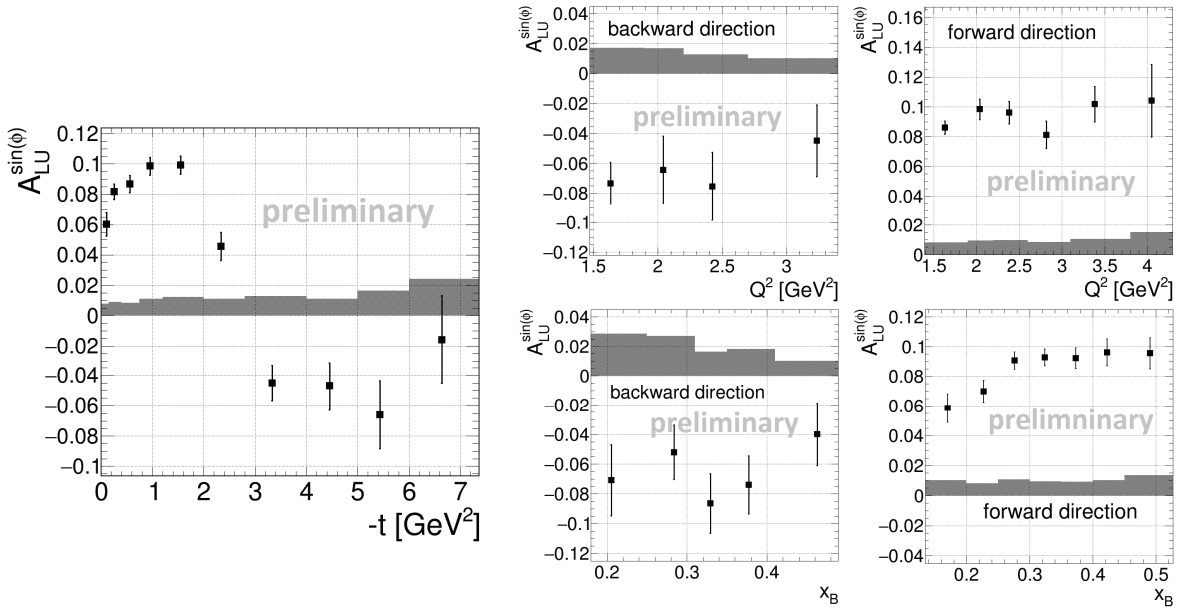

Figure 7. Dependence of $A_{LU}^{\sin(\phi)}$ on -t (left), Q^2 (upper right) and x_B (lower right). The error bars on the data points are poorly statistical, while the shaded area represents the systematic uncertainty. The shown result is preliminary.

A clear transition from positive values up to 0.10 in the forward kinematic region (small -t) to negative values up to -0.06 in the backward kinematic region (large -t) can be observed. As expected the magnitude of $A_{LU}^{\sin(\phi)}$ decreases for very small and large -t values. The smooth transition happens around -t = 3 GeV², which corresponds to a θ_{CM} of 90°. Since the forward kinematic region can be described by GPDs, while the backward kinematic region is described by TDAs, this sign change may indicate the transition between the GPD and TDA based formalisms. The Q^2 and x_B dependence of $A_{LU}^{\sin(\phi)}$ in Fig.8 clearly show, that $A_{LU}^{\sin(\phi)}$ is negative for all Q^2 and x_B bins in backward direction, while it is positive for all bins in forward direction.

In the forward direction, $A_{LU}^{\sin(\phi)}$ can be calculated by the interference of twist-2 longitudinal and twist-3 transverse amplitudes. A prediction for slightly higher Q^2 and W values than in the present

study can be found in [17, 18]. The comparison sows, that the magnitude is slightly higher, but the sign agrees well. In the backward region, a quantitative estimate of the BSA can be made within the collinear factorization approach, employing the dominant leading twist transverse amplitude and a next-to-leading twist subdominant longitudinal amplitude, involving either twist-4 nucleon DAs or twist-4 nucleon-to-pion TDAs, in a similar fashion as done in Ref. [19] for the Pauli to Dirac nucleon form factor ratio. However, calculations are not available yet.

The Q^2 dependence of $A_{LU}^{\sin(\phi)}$ is of particular interest to test the expected $1/Q^2$ scaling, which is related to the onset of the factorisation regime. In the forward direction, no scaling behaviour can be observed, which may hint on a delayed factorisation. Also for the backward direction, no clear evidence for a $1/Q^2$ scaling can be found below 3GeV^2. However the decrease of the last point at a Q^2 of ~$3.3\ \text{GeV}^2$ may hint on an early onset of the factorisation regime, as it was recently reported for the ω backward electroproduction [20-22]. Nevertheless, due to the statistical uncertainty it can not be proven with the present data. High precision measurements become necessary, which will be performed with CLAS12 and in the crossed channel $N\overline{N} \to \gamma^* \pi$, with PADNA at FAIR [23-25].

Acknowledgements

The authors acknowledge theory support and very helpful discussions with B. Pire, K. Semenov-Tian-Shansky and P. Kroll as well as the outstanding efforts of the staff of the Accelerator and the Physics Divisions at Jefferson Lab in making this experiment possible. The work is also supported by DOE grant no: DE-FG02-04ER41309.

References

[1] D. Mueller, D. Robaschik, B. Geyer et al., Fortsch. Phys. **42**, 101 (1994).
[2] A.V. Radyushkin, Phys. Lett. B **380**, 417 (1996).
[3] X. Ji, Phys. Rev. Lett. **78**, 610 (1997).
[4] X. Ji, Phys. Rev. D **55**, 7114 (1997).
[5] K. Goeke, M.V. Polyakov and M. Vanderhaeghen, Prog. Part. Nucl. Phys. **47**, 401 (2001).
[6] M. Diehl, Phys. Rept. **388**, 41 (2003).
[7] A. Belitsky and A. Radyushkin, Phys. Rept. **418**, 1 (2005).
[8] S. Boffi and B. Pasquini, Riv. Nuovo Cim. **30**, 387 (2007).
[9] M. Guidal, H. Moutarde and M. Vanderhaeghen, Rept. Prog. Phys. **76**, 066202 (2013).
[10] K. Kumericki, S. Liuti and H. Moutarde, Eur. Phys. J. A **52**, no. 6, 157 (2016).
[11] L.L. Frankfurt, P.V. Pobylitsa, M.V. Polyakov et al., Phys. Rev. D **60**, 014010 (1999).
[12] B. Pire and L. Szymanowski, Phys. Lett. B **622**, 83 (2005).
[13] B. Pire and L. Szymanowski, Phys. Rev. D **71**, 111501 (2005).
[14] J. P. Lansberg, B. Pire and L. Szymanowski, Phys. Rev. D **75**, 074004 (2007).
[15] M. Guidal, J. M. Laget, and M. Vanderhaeghen, Nucl. Phys. A **627**, 645 (1997).
[16] K. Park et al., CLAS Collaboration, Phys. Lett. B **780** 340345, (2018).
[17] S.V. Goloskokov, P. Kroll, Eur. Phys. J. A **47**, 112 (2011).
[18] S.V. Golosokov, P. Kroll, Eur. Phys. J. C **65:137**, 7 (2010).
[19] A. V. Belitsky, X. d. Ji and F. Yuan, Phys. Rev. Lett. **91**, 092003 (2003).
[20] Wenliang Li, Exclusive Backward-Angle Omega Meson Electroproduction, arXiv: 1712.03214 (2017).
[21] W. Li, G.M. Huber et al., in preparation.
[22] B. Pire, K. Semenov-Tian-Shansky and L. Szymanowski, Phys. Rev. D **91**, no. 9, 094006 (2015).
[23] The PANDA Collaboration, Eur. Phys. J. A **51**, 107 (2015) , DOI: 10.1140/epja/i2015-15107-y
[24] J. P. Lansberg, B. Pire, K. Semenov-Tian-Shansky and L. Szymanowski, Phys. Rev. D **86**, 114033 (2012). Erratum: Phys. Rev. D **87**, no. 5, 059902 (2013).
[25] B. Pire, K. Semenov-Tian-Shansky and L. Szymanowski, Phys. Lett. B **724**, 99 (2013). Erratum: Phys. Lett. B **764**, 335 (2017).